Synthesis and reactivity of N@C_{60}O

Mark A. G. Jones,*[a] David A. Britz,[ad] John. J. L. Morton,[ab] Andrei N. Khlobystov,[ac] Kyriakos Porfyrakis,[a] Arzhang Ardavan[b] and G. Andrew D. Briggs[a]

Received 25th January 2006, Accepted 7th March 2006
First published as an Advance Article on the web 24th March 2006
DOI: 10.1039/b601171c

The endohedral fullerene epoxide N@C_{60}O was synthesised, isolated by High Performance Liquid Chromatography (HPLC), and characterised by Electron Spin Resonance (ESR). This nitrogen radical displays predominantly axial symmetry characteristics as expected for a monoadduct, evidenced by a zero-field splitting D parameter of 6.6 MHz and an E parameter of 0.5 MHz in powder at 77 K. Photo- and thermally-activated silencing of the nitrogen radical were observed, the latter showing the evolution of a new spin signal during heating at 100 °C. We suggest that loss of nitrogen spin is due to coupling with a radical formed by opening of the epoxide ring. This implies that the reaction of $C_{60}O$ with C_{60} in the solid state proceeds *via* a radical, rather than ionic, intermediate.

Introduction

There is strong evidence that a nitrogen atom incarcerated in a fullerene cage, N@C_{60}, is physically isolated from its environment. Only 2% of the nitrogen electron spin density resides on the fullerene cage,[1] as suggested by ^{13}C Electron Nucleus Double Resonance (ENDOR) measurements. In pulsed Electron Spin Resonance (ESR), N@C_{60} has shown electron spin lifetimes T_1 of hundreds of seconds and T_2 of 240 μs,[2] the longest observed for a molecular radical. The remarkable spin lifetimes of N@C_{60} make it an interesting candidate material for electron spin-based quantum information processing (QIP).[3] Many proposals for fullerene-based quantum computers require functionalization of the fullerene cage in such a way that the fullerenes assemble into periodic structures on a surface[3] or in a nanotube.[4,5] Any viable steps towards a fullerene-based quantum computer require studying the effect on the spin properties of the nitrogen atom due to intentional and incidental changes of the cage.

The first examples of N@C_{60} functionalization were the mono and hexaddition of :C(COOEt)$_2$ carbene to a C_{60}/N@C_{60} mixture.[6] The fullerene dimer N@C_{60}–C_{60} has also been formed by vibrational milling.[7] In the carbene functionalization, N@C_{60} appears to be as reactive as C_{60}, which is ascribed to the small interaction between the nitrogen and the fullerene cage.

Fullerenes readily oxidize under a variety of conditions, and $C_{60}O$ tends to naturally form under ambient conditions. $C_{60}O$ can further react to form larger arrays, including dimers[8] and polymers.[9] N@C_{60}O is therefore also a useful precursor for molecular architectures for QIP, as well as forming incidentally during chemical processing. We report here a study on epoxidation of N@C_{60} and the purification and reactivity of the product, N@C_{60}O, as well as attempts to synthesize the dimer N@C_{60}OC_{60}.

Results and discussion

Synthesis and purification

N@C_{60} was produced using the ion implantation method.[10] The product was enriched using single injection High Performance Liquid Chromatography (HPLC)[11] until the sample was approximately 10^{-3} N@C_{60}/C_{60}, **1**, (mol mol^{-1}). **1** was oxidized using the procedure similar to that used by Murray and Iyanar (Scheme 1).[12] Specifically, we mixed 5 mg of **1** with 1 mg MeO_3Re in 5 mL of toluene. After dissolving **1** and MeO_3Re, 13.1 mg of urea/H_2O_2 was added, and the mixture was stirred under ambient conditions for 12 h. Upon completion of the reaction, the crude product was filtered, and the filtrate was concentrated yielding a mixture of N@C_{60}O/C_{60}O, **2**, and higher oxides, **3**, as well as unreacted **1**. The crude product was purified by HPLC (Fig. 1).

ESR characterisation

The as-produced N@C_{60}/C_{60} mixture **1** has an ESR signal consisting of a triplet of sharp peaks, resulting from the hyperfine splitting of the nitrogen S = 3/2 electron spin transitions by the I = 1 ^{14}N nucleus. This signal entirely originates from N@C_{60}; C_{60} is spin-silent. The lines are

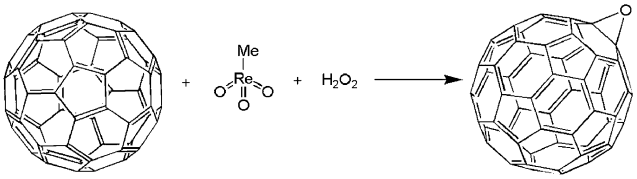

Scheme 1 The epoxidation of **1** (C_{60}) to form **2** (C_{60}O) using the procedure of Murray and Iyanar.[12]

[a] *Department of Materials, Oxford University, Parks Road, Oxford, UK OX1 3PH. E-mail: mark.jones@materials.ox.ac.uk; Fax: +44 1865 273730*
[b] *Clarendon Laboratory, Oxford University, Parks Road, Oxford, UK OX1 3PU*
[c] *School of Chemistry, Nottingham University, Nottingham, UK NG7 2RD*
[d] *Eikos Inc., 2 Master Drive, Franklin, MA, USA*

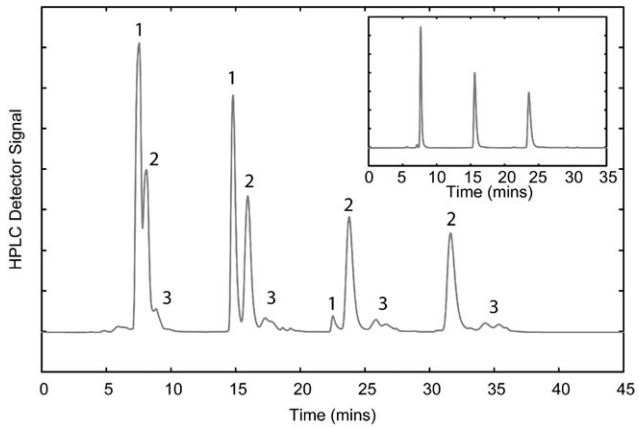

Fig. 1 Recycling HPLC separation of $C_{60}O$ from C_{60}. Peak **1** is C_{60}, Peak **2** is $C_{60}O$. After the second and third passes, Peak **1** was collected. After the final pass, Peak **2** was collected separately from the later peaks (higher oxides **3**). The inset shows **2** passing through the HPLC in recycling mode, note the absence of additional features, indicating the high purity for fraction **2**.

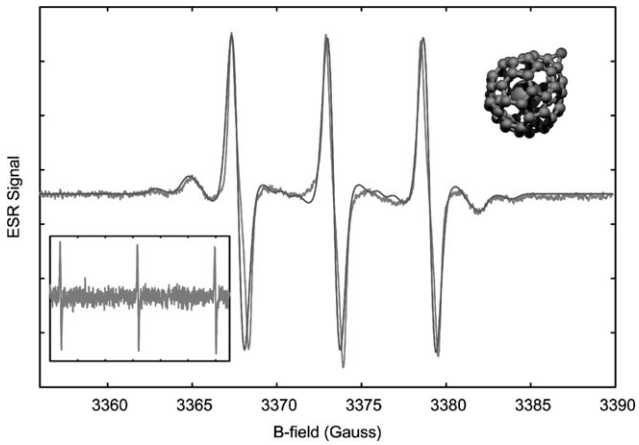

Fig. 2 X-band ESR experimental spectrum and simulated spectrum of $N@C_{60}O$ powder at 77 K, acquired with a modulation amplitude of 1000 mG. Inset shows same spectral region acquired in toluene solution at 77 K. Fit to powder spectrum (smooth line) is simulated using line parameters consistent with observed $N@C_{60}$ (g = 2.003, A = 15.45 MHz) and instrumental parameters of ν = 9.4583 GHz, with Lorentzian widths of 0.75 G. Close fit was achieved with a D term of 6.6 MHz, and an E term of 0.5 MHz.

unusually narrow by virtue of the high symmetry of the $N@C_{60}$ system; if the symmetry of this system is perturbed by functionalization with a polar functional group (such as oxygen), axial (D) and rombohedral (E) terms should enter the spin Hamiltonian, leading to a zero-field splitting (ZFS) and the appearance of satellite peaks in the ESR spectrum.[7,14] When freshly purified $N@C_{60}O/C_{60}O$ **2** was examined by ESR in degassed CS_2, it was found to have a linewidth of 8 mG. The hyperfine coupling (15.7 MHz) and g-factor (2.003) were indistinguishable from **1**, showing that the presence of the local dipole due to the epoxide group does not substantially perturb the nitrogen wavefunction. However, if the asymmetry effects due to the functional group are to be observed, the rotational motion of the fullerene must be reduced, for example by cooling the sample.[18]

We evaporated the solvent under vacuum at room temperature to form a powder sample. At room temperature, the spectrum of **2** was indistinguishable from **1** under all conditions. However, at 77 K, satellites of each peak became apparent (Fig. 2). Fitting a simulation to this spectrum allowed determination of the axial ZFS term, D = 6.6 MHz, with a rombohedral term, E = 0.5 MHz. This is consistent with the predominantly axial symmetry of the oxide. Our observation that no ZFS is observable in **2** at room temperature is expected, since $C_{60}O$ rotates freely in the crystalline state above 270 K, as demonstrated by Meingast *et al*. using X-ray crystallography.[13] This ZFS is comparable to that observed in $N@C_{61}(COOEt)_2$ (D = 5.9 MHz)[14] and smaller than that observed in $N@C_{60}$–C_{60} (D = 14.0 MHz).[7] This trend is consistent with that observed in ^{3}He NMR chemical shifts of the analogous $^3He@C_{60}O$,[15] $^3He@C_{61}(COOEt)_2$,[16] and $^3He@C_{60}$–C_{60}.[17]

$N@C_{60}O$ spin loss

We found that a sample of **2** stored in degassed CS_2 and left exposed to ambient light showed a significant loss of ESR signal intensity. This observation led us to test the stability of $N@C_{60}O$. We prepared samples of **2** in toluene solution, CS_2 solution, and as a powder. The samples were monitored by ESR over several days while being maintained at cryogenic and room temperatures and exposed to ambient room light and dark conditions.

From these experiments, we observed that **2** is stable in the dark at room temperature. However, a sample in toluene exposed to ambient light exhibited a linear decay of ESR intensity with a half life of approximately two days. Recently, 1,1,2,2-tetramesityl-1,2-disilirane was added to $C_{60}/N@C_{60}$ using a photochemical reaction.[18] The relatively lower spin concentration in the functionalized product was ascribed to $N@C_{60}$ having lower photochemical reactivity than C_{60}. In light of our observations here, we suggest the possibility that these results may alternatively be explained by comparable photoreactivity of $N@C_{60}$ and C_{60} towards 1,1,2,2-tetramesityl-1,2-disilirane together with low photostability of $N@C_{60}$ in toluene. The functionalized fullerenes or precursor fullerenes may have been losing nitrogen spin activity due to exposure to the light of the photoirradiation source.

To study epoxide reactivity using a well-known dimerisation reaction, we attempted to react **2** with C_{60} to make a fullerene dimer, **4** (Scheme 2). The dimerisation proceeds by ring opening of the epoxide and formation of a furan bridge between the two cages.[19] $C_{120}O$ can form naturally in fullerene powder that has been exposed to air at room temperature.[20] We have found that fullerene epoxides efficiently react with C_{60} at temperatures as low as 100 °C. By heating a solid state mixture of **2** with a tenfold excess of C_{60} at 100 °C in an evacuated ESR tube, we were able to monitor the reaction evolution. Although **2** freely rotates in all directions in the solid state at room temperature, **4** would have several degrees of rotation that are forbidden, permitting the observation of asymmetry effects, with the ESR spectrum showing the characteristic

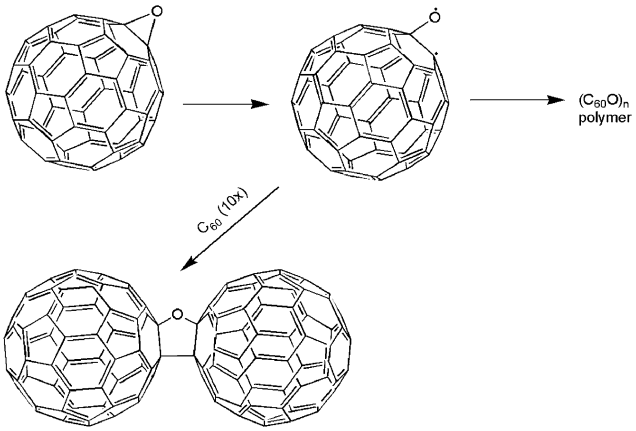

Scheme 2 The polymerisation or dimerisation of **2** ($C_{60}O$) *via* opening of the epoxide ring and formation of associated radicals.

satellite lines growing over time as **2** converts to **4**.[7] The time-resolved ESR behaviour of these lines would thus allow the dynamics of the reaction to be studied.

After the reaction mixture had been flame-sealed and then left under vacuum and maintained at room temperature for 5 h, a single ESR peak was observed to emerge slightly downfield of the central N@C_{60} peak with $g = 2.006$. This feature was broader than the nitrogen peaks and had no further structure. After heating to 100 °C (Fig. 3), the intensity of the broad feature grew and the intensity of the nitrogen triplet signal decreased exponentially with time (Fig. 4). No features of the spectrum that would indicate a ZFS from nitrogen-containing dimers[7] were found at any point during the reaction. After six days, the reaction mixture was dissolved in toluene and the products were isolated by HPLC. Unreacted **2** was found to contain all spins associated with endohedral nitrogen after the reaction completion, whereas **4** was spin silent. N@C_{60}O therefore appears less thermally stable than N@C_{60} and N@$C_{61}(COOEt)_2$.[21] Signal loss for N@C_{60}O at such low temperatures may be explained by a lower barrier for loss of nitrogen spin, relative to N@C_{60} and N@$C_{61}(COOEt)_2$.[22]

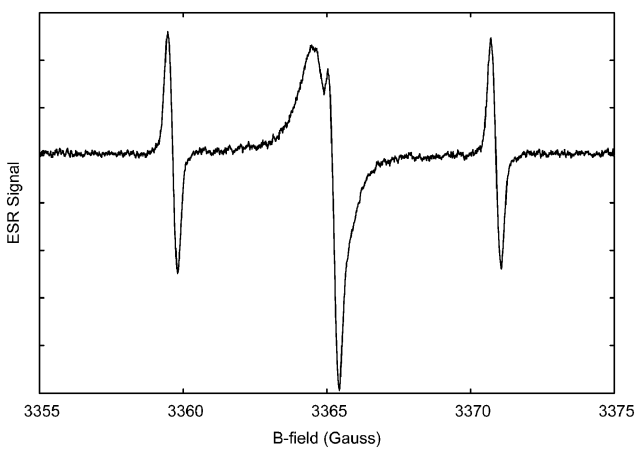

Fig. 3 ESR spectrum of dimerization reaction mixture after 16 h at 100 °C. In addition to the nitrogen triplet, there is also a broad resonance slightly downfield from the center of the triplet.

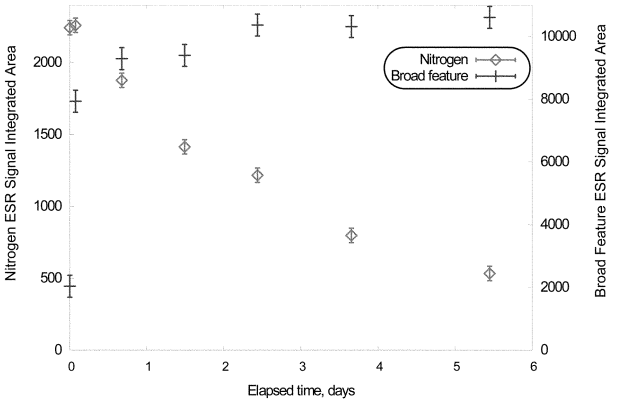

Fig. 4 ESR intensity of broad feature and nitrogen triplet during dimer reaction, showing rapid evolution of broad feature and decline of nitrogen signal.

$C_{60}O$ radical formation in the solid state

To investigate the relationship between the evolution of the broad peak and the decrease in signal of the nitrogen triplet, a variety of samples incorporating $C_{60}O$ were observed under the conditions of the dimerization reaction. Both pure $C_{60}O$ **5** and $C_{60}O$ with a tenfold excess of C_{60} **6** were studied, **5** forming $(C_{60}O)_n$ polymer **7** under these conditions, and **6** forming predominantly dimer $C_{120}O$, **4**. The reactions were carried out in pyrex ESR tubes, with one set of samples open to the air, the other under an inert nitrogen atmosphere. The evolution of each sample was regularly monitored using ESR.

During the reactions involving **5** and **6**, a broad ESR peak similar to that observed for the reaction of **2** (Fig. 3) evolved in all the samples. This feature showed a rapid initial gain in spin activity which plateaued at a constant level after 24 h for all samples except **6** in air, which continued to show monotonic growth after three days without sign of saturation. We attribute this generation of radicals in **6** in air to the oxidation of fullerene cages from atmospheric oxygen, giving a signal similar to that previously seen in solid fullerene exposed to oxygen at room temperature.[23]

Samples of **5** showed saturation at a signal level approximately twenty times greater per unit mass of $C_{60}O$ than the **6** inert sample. The **6** samples showed broadening of the ESR line to ~1 G, and the **5** samples showed broadening to ~2 G, ascribed to the magnetic dipole–dipole induced broadening with increasing radical concentration. When the number of spins in sample **5** was compared to a reference of the well-characterized radical DPPH it was found that approximately one in ten fullerenes hosts an electron spin.

On elevation of the temperature to 250 °C, the spin signal decreased markedly for all samples within 12 h. The spin signal of the **6** sample in air initially peaked sharply by a further 75% of the value previous to heating to 250 °C, and then decreased after 12 h, presumably from further cage oxidation, to full sample decay. Spin signals for the inert samples reduced by two orders of magnitude over 4 days. At 250 °C in an inert environment, fullerene cages are stable, so any loss of the broad feature intensity is likely due to an annealing and reorganization of the crystal structure of **5** and **6**.

It is evident from the generation and decay of the ESR signal intensity that the broad feature is not associated exclusively with the $N@C_{60}O$ system, but can be attributed to metastable radicals forming in the fullerene crystal lattice due to the thermally induced opening of the epoxide ring in $C_{60}O$ or $N@C_{60}O$. The opening of the epoxide ring provides a possible mechanism for the nitrogen spin to be quenched by a strong spin–spin interaction or reaction with this radical. Fast quenching of photoexcited $C_{60}O$ triplet states compared with the equivalent states in C_{60} has already been observed, and associated with rapid opening and closing of the epoxide ring.[24]

The weakest bonds in $C_{60}O$ are those associated with the epoxide ring, as these bonds are highly strained. At 100 °C, the opening of the epoxide ring is the mechanism for the dimer $C_{120}O$ formation.[13,19] Usually, the open epoxide ring reacts when $C_{60}O$ rotates to an orientation where the open epoxide ring can react with a double bond on another fullerene cage. However, when one $C_{60}O$ is surrounded by other $C_{60}O$ molecules, the freely-rotating $C_{60}O$ can become locked along one axis due to the reaction with a neighbouring $C_{60}O$ to form $C_{120}O_2$. This hinders the rotation of an open epoxide ring. Complete rotational locking can occur if another fullerene oxide reacts with the $C_{120}O_2$, leading to removal of all degrees of rotational freedom. In this case, if this reaction occurred before the epoxide ring could react, and with the epoxide ring located in an unreactive interstitial site, the open epoxide ring could host a metastable radical, leading both to the observed spin signal (Fig. 5) and a potential mechanism for the decay of the nitrogen spin through reaction with this radical. It has already been suggested that $C_{60}O$ reacts with C_{60} to form a dimer by either a radical or ionic intermediate associated with the opened epoxide ring,[19] and our observation supports the hypothesis of the existence of a radical intermediate. We performed a Monte-Carlo simulation to determine the statistics of rotational hindrance as a function of the ratio of $C_{60}O$ to C_{60}. This model accounts for the experimentally observed factor of 20 difference in saturation radical concentration between samples **5** and **6**.

As the temperature is raised further to 250 °C, the furan ring bridging neighboring fullerene cages can open, unlocking the molecular rotation and permitting a previously locked epoxide ring to reach a reactive site, this accounts for the decrease in signal on temperature elevation.

Based on our observations of loss of spin from $N@C_{60}O$ upon exposure to light or heat, we speculate on a mechanism for loss of the nitrogen spin (Fig. 6). The epoxide ring opens upon heating and the radical on the fullerene cage couples with the nitrogen atom, displacing it from the centre. The nitrogen atom may pass from the inside to the outside of the cage *via* a C–O–C–N four membered ring. We suggest that this structure could proceed to a fullerene cage with a C–C–O–N four membered ring, essentially an N–O molecule bonded outside the cage. The radical on the N–O molecule can react with a neighbouring cage or with solvent trapped in the crystal, silencing the spin.[25] This proposed mechanism may form the basis of an *ab initio* model of the loss of nitrogen spin in $N@C_{60}$.[26]

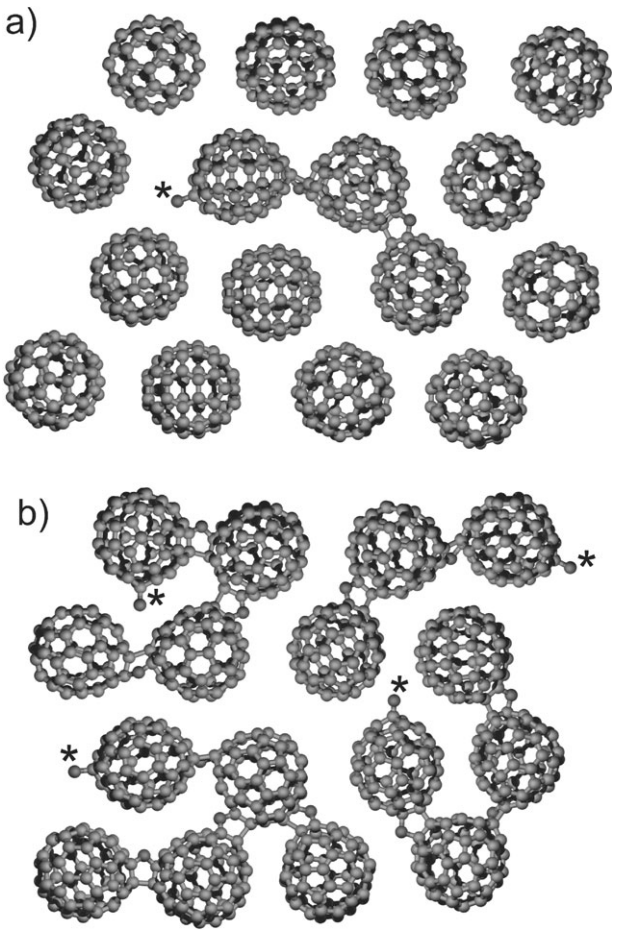

Fig. 5 Schematic diagram of close-packed (a) $C_{60}O/C_{60}$ mixture and (b) pure $C_{60}O$, showing how radicals can be formed by trapping opened epoxide rings in interstitial sites. Sites hosting radicals are indicated by stars. The structures are illustrative and are not intended to show actual proportions of spins or of actual locked structures.

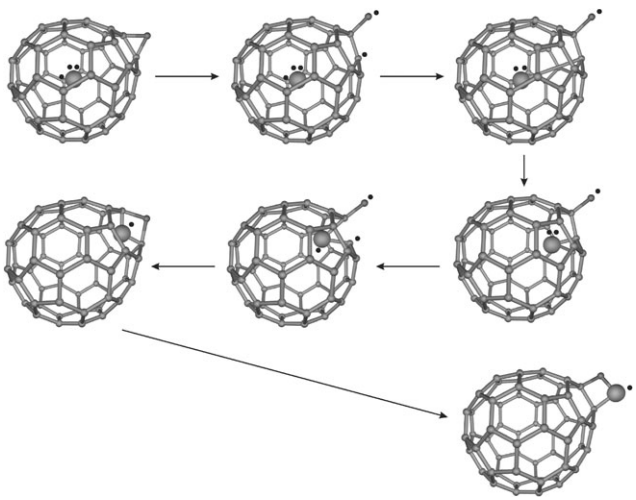

Fig. 6 Possible example mechanism for loss of nitrogen spin. Unpaired electrons are indicated by black dots. Nitrogen is enlarged for ease of view.

Conclusion

We have synthesised and isolated $N@C_{60}O$ and studied its thermal and photoreactivity. We demonstrated that $N@C_{60}O$ powder shows dynamic merohedral disorder at room temperature, which is frozen out with decreased temperature. At 77 K, the $N@C_{60}O$ powder shows characteristic axial symmetry effects in its ESR spectrum due to ZFS terms $D = 6.6$ MHz and $E = 0.5$ MHz. $N@C_{60}O$ is stable in the solid state and in toluene in the dark, but unstable when exposed to ambient light and heat. We also investigated a mechanism for spin-loss during dimerisation by time-resolved ESR of this reaction, and observed the appearance of a stable radical species in the reaction mixture, hypothesised to be associated with the opening of the epoxide ring and responsible for quenching the nitrogen spin. This phenomenon is worthy of further study as a unique radical system. Any future application of $N@C_{60}$ should consider the possibility of the fullerene oxidising and subsequently losing nitrogen spin.

Experimental

$N@C_{60}$ was produced using the ion implantation method.[10] The product was enriched using single injection HPLC[11] until the sample was approximately 10^{-3} $N@C_{60}/C_{60}$, **1**, (mol mol^{-1}). **1** was oxidized using the procedure similar to that used by Murray and Iyanar (Scheme 1).[12] Specifically, we mixed 5 mg of **1** with 1 mg MeO_3Re in 5 mL of toluene. After dissolving **1** and MeO_3Re, 13.1 mg of urea/H_2O_2 was added, and the mixture was stirred under ambient conditions for 12 h. Upon completion of the reaction, the crude product was filtered and the filtrate was concentrated yielding a mixture of $N@C_{60}O/C_{60}O$, **2**, and higher oxides, **3**, as well as unreacted **1**. To purify $N@C_{60}O$ and $C_{60}O$ (**2**) from **1**, HPLC was employed (Buckyprep-M 20 mm diameter $\times$ 250 mm, toluene eluent, 18 mL min^{-1}, 312 nm detector). Generally, a concentrated solution of the crude product was injected, and a peak, known to be **1**, appeared at 7.0 min after injection. A peak known to be **2** begins to appear after at 7.6 min. Therefore, to reduce sample size for future HPLC passes, **1** was collected from 7.0 to 7.6 min. Several other peaks appeared after **2**, attributed to higher fullerene oxides, $C_{60}O_n$. These peaks were collected with **2** in a separate flask from 7.6 min to 12.5 min. The flask containing **2** was again concentrated and re-injected into the HPLC. Before recycling, **1**, which has a long tail that overlapped with the **2** peak from the previous injection, was collected. The sample was sent through the column four times in recycling mode, which improved separation of **2** and the higher fullerene oxides. After the third pass, $C_{60}O_3$ and higher oxides were cut out and collected. After the fourth pass, **2** was collected separately from $C_{60}O_2$ **3** (two peaks). In order to minimize the amount of **3** in the **2** fraction, the **3** peaks were conservatively collected at 33.3 min. Both the **3** and higher fullerene oxide samples were concentrated and reinjected into the HPLC, and **2** was collected from both samples and added to the flask containing $C_{60}O$. Finally, **2** was injected into the HPLC to remove any possible remaining **1**. The $C_{60}O$ fraction was recycled three times, and the peak was cut in half after the third pass through the column and collected separately. The purity of all samples was checked with MALDI-TOF (Matrix-Assisted Laser Desorption/Ionization Time-Of-Flight) mass spectrometry and UV-visible absorption spectroscopy.

In HPLC, $N@C_{60}$ generally elutes after C_{60}, by about 0.15 min on a HPLC Buckyprep-M column, and $C_{60}O$ elutes about 0.6 min after C_{60} under the same conditions (Fig. 1). There is substantial overlap between $N@C_{60}$ and $C_{60}O$ peaks, but the two are distinguishable and therefore in principle separable. To demonstrate that $N@C_{60}$ had not tailed into $C_{60}O$, we examined the first and second half of the purified HPLC peak identified as $N@C_{60}O/C_{60}O$, **2**, with ESR. The first half had no spins, whereas the second half of the peak showed that signal usually associated with endohedral nitrogen fullerenes. The spin concentration was about half of the unreacted and recovered **1** and half what would be expected if C_{60} and $N@C_{60}$ were converted at equal rates to $C_{60}O$ and $N@C_{60}O$, respectively. Because of the procedure to isolate **2**, it is unlikely that the $N@C_{60}O$ was lost in some other fraction of the sample.

To form $C_{120}O$, **4**, 500 μg of **2** was dissolved in CS_2 with 5 mg of C_{60}, and the mixture was dried in a Pyrex ESR tube. The sample was evacuated for 5 h at room temperature in the dark to remove residual solvent. The tube then was sealed under vacuum and the ESR signal measured to establish endohedral nitrogen signal strength before heating. The sample was kept at 100 °C for several days and ESR spectra were measured at regular intervals. After six days, the reaction mixture was dissolved in toluene and the products were separated by HPLC. The spin signal remaining in the bulk reaction mixture was found in the unreacted **2**, whereas **4** was spin silent.

Computational

For the pure $C_{60}O$ case, we assume that in each time interval, every unlocked (*i.e.* free- or singly-bonded) $C_{60}O$ bonds with a nearby $C_{60}O$. Once a trimer has formed, it is considered locked due to total loss of free rotation. The trimer, $C_{180}O_3$, will host a radical only if it has been locked with the unreacted epoxide group oriented in an interstitial site. Therefore, this case can be directly compared with the low-concentration case described below, because trimers are considered the minimal oligomeric structure hosting a radical; a $C_{120}O_2$ dimer still has rotational freedom about its long axis, allowing further reaction of the epoxide on one cage. Reaction probabilities are determined only by time-ordering of bond formation and proportion of unreactive orientations for an epoxide group. Therefore, between the two extremes of $C_{60}O$ concentration, the reaction probability is a constant factor. From our experimental results, we find that one in ten fullerene cages (10%) in the pure $C_{60}O$ powder hosts a radical, which gives us the reaction probability for a given $C_{60}O$ bonding with a nearest neighbour. This factor becomes a fixed multiplier for the absolute spin concentration of the pure $C_{60}O$ powder and of the 10 : 1 $C_{60}/C_{60}O$ powder.

To compare the radical proportions of the 10 : 1 $C_{60}/C_{60}O$ and pure $C_{60}O$, a Monte-Carlo model was developed which considers the bonding structure associated with a single $C_{60}O$ molecule in an FCC lattice, deemed the master $C_{60}O$. The nearest-neighbour and next-nearest-neighbour sites in the

FCC lattice were populated so that a given proportion of the lattice sites hosted $C_{60}O$ and the remainder C_{60}. Each nearest-neighbour site hosting a $C_{60}O$ was randomly bonded *via* its epoxide ring to one of its 12 nearest neighbours. If no $C_{60}O$ bonded to the central master $C_{60}O$, then the master was regarded as unlocked. If two or more $C_{60}O$ molecules bonded to the master, the structure was regarded as locked due to total loss of free rotation of the master. If only one $C_{60}O$ bonded to the master, then the 11 nearest neighbours of the bonding $C_{60}O$ were likewise considered for bonding. If any one of these bonded with the $C_{60}O$ under consideration, then a trimer was created with an epoxide ring on the master, and the structure was considered locked. Averaging over several runs of this Monte-Carlo produced a figure between 6% and 7% for the proportion of potentially locked epoxide.

Therefore, the percentage of trimers (100% for pure $C_{60}O$ powder and 6.5% for 10 : 1 $C_{60}/C_{60}O$ powder) multiplied by the probability of hosting a radical (10% for both cases) gives the percentage of radicals per $C_{60}O$ in each sample (10% for pure $C_{60}O$ powder and 0.65% for 10 : 1 $C_{60}/C_{60}O$ powder). These figures are consistent with the experimentally observed radical concentrations at steady state, which show a factor of approximately twenty difference in spin concentration between the cases.

Acknowledgements

We thank Alexei Tyryshkin for his valuable assistance. The Oxford-Princeton Link helped support this project. This research is part of the QIP IRC www.qipirc.org (GR/S82176/01). G. A. D. B. thanks EPSRC for a Professorial Research Fellowship (GR/S15808/01). A. A. is supported by the Royal Society. A. K. thanks The Leverhulme Trust and The Royal Society. D. A. B. thanks the Overseas Research Scholarship scheme. M. A. G. J. is supported by an EPSRC DTA studentship. J. J. L. M. thanks St. John's College, Oxford for a Junior Research Fellowship. The authors are also grateful to the EPSRC National Mass Spectrometry Service Centre at the University of Swansea, Wales.

References

1 N. Weiden, H. Kass and K.-P. Dinse, *J. Phys. Chem. B*, 1999, **103**, 9826.
2 J. J. L. Morton, A. M. Tyryshkin, A. Ardavan, K. Porfyrakis, S. A. Lyon and G. A. D. Briggs, *J. Chem. Phys.*, 2006, **124**, 014508.
3 W. Harneit, *Phys. Rev. A*, 2002, **65**, 032322.
4 A. Ardavan, M. Austwick, S. C. Benjamin, G. A. D. Briggs, T. J. S. Dennis, A. Ferguson, D. G. Hasko, M. Kanai, A. N. Khlobystov, B. W. Lovett, G. Morley, R. A. Oliver, D. G. Pettifor, K. Porfyrakis, J. H. Reina, J. H. Rice, J. D. Smith, R. A. Taylor, D. A. Williams, C. Adelmann, H. Mariette and R. J. Hamers, *Philos. Trans. R. Soc. London, Ser. A*, 2003, **361**, 1473.
5 J. Twamley, *Phys. Rev. A*, 2003, **67**, 052318.
6 B. Pietzak, M. Waiblinger, T. Almeida Murphy, A. Weidinger, M. Hiihne, E. Dietel and A. Hirsch, *Chem. Phys. Lett.*, 1997, **279**, 259.
7 B. Goedde, M. Waiblinger, P. Jakes, N. Weiden, K.-P. Dinse and A. Weidinger, *Chem. Phys. Lett.*, 2001, **334**, 12.
8 S. Lebedkin, S. Ballenweg, J. Gross, R. Taylor and W. Kraetschmer, *Tetrahedron Lett.*, 1995, **36**, 4971.
9 D. A. Britz, A. N. Khlobystov, K. Porfyrakis, A. Ardavan and G. A. D. Briggs, *Chem. Commun.*, 2005 (1), 37.
10 T. A. Murphy, Th. Pawlik, A. Weidinger, M. Hohne, R. Alcala and J. M. Spaeth, *Phys. Rev. Lett.*, 1996, **77**(6), 1075–1078.
11 M. Kanai, K. Porfyrakis, G. A. D. Briggs and T. J. S. Dennis, *Chem. Commun.*, 2004 (2), 210.
12 R. W. Murray and K. Iyanar, *Tetrahedron Lett.*, 1997, **38**, 335.
13 C. Meingast, G. Roth, L. Pintschovius, R. H. Michel, C. Stoermer, M. M. Kappes, P. A. Heiney, L. Brard, R. M. Strongin and A. B. Smith, *Phys. Rev. B*, 1996, **54**, 124.
14 E. Dietel, A. Hirsch, B. Pietzak, M. Waiblinger, K. Lips, A. Weidinger, A. Gruss and K.-P. Dinse, *J. Am. Chem. Soc.*, 1999, **121**, 2432.
15 A. B. Smith III, R. M. Strongin, L. Brard and W. J. Romanow, *J. Am. Chem. Soc.*, 1994, **116**, 10831.
16 M. Saunders, R. J. Cross, H. A. Jimenez-Vazquez, R. Shimshi and A. Khong, *Science*, 1996, **271**, 1693.
17 K. Komatsu, G.-W. Wang, Y. Murata, T. Tanaka and K. Fujiwara, *J. Org. Chem.*, 1998, **63**, 9358.
18 T. Wakahara, Y. Matsunaga, A. Katayama, Y. Maeda, M. Kako, T. Akasaka, M. Okamura, T. Kato, Y.-K. Choe, K. Kobayashi, S. Nagase, H. Huange and M. Ata, *Chem. Commun.*, 2003 (23), 2940.
19 A. B. Smith III, H. Tokuyama, R. M. Strongin, G. T. Furst, W. J. Romanow, B. T. Chait, U. A. Mirza and I. Haller, *J. Am. Chem. Soc.*, 1995, **117**, 9359.
20 R. Taylor, M. P. Barrow and T. Drewello, *Chem. Commun.*, 199822), 2497.
21 M. Waiblinger, K. Lips, W. Harneit, A. Weidinger, E. Dietel and A. Hirsch, *Phys. Rev. B*, 2001, **64**(15), 159901.
22 M. Waiblinger, K. Lips, W. Harneit, A. Weidinger, E. Dietel and A. Hirsch, *Phys. Rev. B*, 2001, **63**(4), 045421.
23 P. Paul, K.-C. Kim, D. Sun, P. D. W. Boyd and C. A. Reed, *J. Am. Chem. Soc.*, 2002, **124**, 4394.
24 G. Agostini, C. Corvaja and L. Pasimeni, *Chem. Phys.*, 1996, **202**, 349.
25 K. Lips, M. Waiblinger, B. Pietzak and A. Weidinger, *Phys. Status Solidi A*, 2000, **177**, 81.
26 H. Mauser, A. Hirsch, N. J. R. van Eikema Hommes, T. Clark, B. Pietzak, A. Weidinger and L. Dunsch, *Angew. Chem., Int. Ed. Engl.*, 1997, **36**, 2835.

